for an appropriate structure factor can determine, through phase determining formulas, the choice of the proper alternative for the remaining structure factors of interest.

When the probabilities or variances do not permit the application of phase determining relations in a step-by-step fashion by giving definitive choices between the alternative values for the phases, it is possible to proceed according to the suggestion of Coulter (1965). In his procedure a large amount of preliminary phase information can be assembled, since the phases of pure real and pure imaginary structure factors are determined by a single isomorphous substitution, and in many instances the ambiguous alternatives for the complex structure factors are not widely separated, thus permitting the averages of their alternative phase values, given by the phase of the substitution, to be used as a starting point. This preliminary phase information can then be refined and extended by use of formula (4.2) below.

When the probability measures are high enough, the phase determination can proceed in a step-by-step fashion by employing appropriate phase determining formulas for the noncentrosymmetric space groups. An advantage in proceeding in this way is that it would be initially possible to evaluate the phases associated with the largest E-magnitudes, even though the ambiguous values for the associated phases were widely separated. The phase determining formulas are

$$\varphi_{\mathbf{h}} \approx \langle \varphi_{\mathbf{k}} + \varphi_{\mathbf{h}-\mathbf{k}} \rangle_{\mathbf{k}_r}, \tag{4.1}$$

and

$$\tan \varphi_{\mathbf{h}} \approx \frac{\sum_{\mathbf{k}} |E_{\mathbf{k}} E_{\mathbf{h}-\mathbf{k}}| \sin (\varphi_{\mathbf{k}} + \varphi_{\mathbf{h}-\mathbf{k}})}{\sum_{\mathbf{k}} |E_{\mathbf{k}} E_{\mathbf{h}-\mathbf{k}}| \cos (\varphi_{\mathbf{k}} + \varphi_{\mathbf{h}-\mathbf{k}})}, \tag{4.2}$$

where the $E_{\mathbf{k}}$ represent normalized structure factors whose phases are $\varphi_{\mathbf{k}}$ and the symbol $\mathbf{k}_r$ implies that the average extends only over those vectors, $\mathbf{k}$, associated with large $|E_{\mathbf{k}}|$ values. The application of these formulas in connection with the symbolic addition procedure has been discussed elsewhere (Karle & Karle, 1964, 1966). It is suggested that the symbolic addition procedure be followed in direct combination with the information from the isomorphous substitution. Clearly the addition of this latter information reduces the problem from determining the value of a phase from the continuous range of $-\pi$ to $+\pi$ to that of choosing between only two possible values permitted by the interpretation of the substitution. Measures ot the variance (Karle & Karle, 1966, equation (3.33) and Fig. 2) may be employed in order to evaluate the reliability of the contributors in (4.1). In this way a set of phases may be generated in a stepwise fashion.

References

BIJVOET, J. M. (1952). Conference on Computing Methods and the Phase Problem in X-ray Crystal Analysis: Penn. State College. p. 84.

BOKHOVEN, C., SCHOONE, J. C. & BIJVOET, J. M. (1951). *Acta Cryst.* **4**, 275.

COULTER, C. L. (1965). *J. Mol. Biol.* **12**, 292.

HAUPTMAN, H. & KARLE, J. (1953). *Solution of the Phase Problem. I. The Centrosymmetric Crystal.* A.C.A. Monograph No. 3. Pittsburgh Polycrystal Book Service.

International Tables for X-ray Crystallography (1952). Vol. I. Birmingham: Kynoch Press.

KARLE, I. L. & KARLE, J. (1964). *Acta Cryst.* **17**, 835.

KARLE, J. & HAUPTMAN, H. (1956). *Acta Cryst.* **9**, 635.

KARLE, J. & HAUPTMAN, H. (1959). *Acta Cryst.* **12**, 404.

KARLE, J. (1964). *Advances in Structure Research by Diffraction Methods,* Vol. I. Edited by R. Brill. New York: Interscience Publishers.

KARLE, J. & KARLE, I. L. (1966). *Acta Cryst.* To be published.

WOOLFSON, M. M. (1954). *Acta Cryst.* **7**, 61.

Acta Cryst. (1966). **21**, 276

Some Growth Features on (111) Faces of Natural Diamonds

BY FEDERICO BEDARIDA* AND HIROSHI KOMATSU

Physics Department, Royal Holloway College, Englefield Green, Surrey, England

(*Received* 1 *November* 1965)

Some particular features on the (111) faces of a diamond are reported. They are vicinal faces built up by extremely thin growth layers. A growth mechanism is suggested.

Introduction

The crystal studied was picked from among some hundreds of natural diamonds from South Africa. It is a tabular twinned octahedron modified to a rounded hexaoctahedron on the sides, and the crystal is so flattened that only two octahedral faces, *viz.* (111) and $(\bar{1}\bar{1}\bar{1})$, appear as well as curved (*hkl*) type faces.

A small portion of the crystal had been chipped off (Fig. 1). This diamond weighs 0·58 carat, is transparent and as far as can be seen under the microscope has no

* Present address: Istituto di Mineralogia, Università di Genova, Via Leon Battista Alberti 4, Genova, Italy.

Fig. 1. The diamond, twinning on (111) face ($\times 8$).

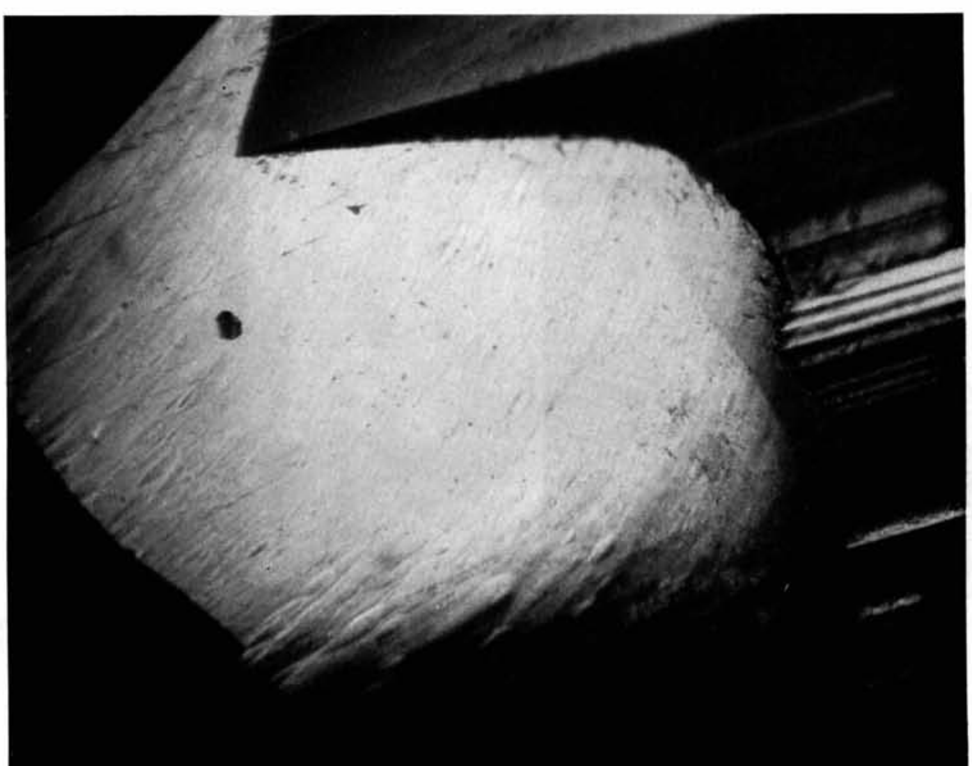

Fig. 2. The surface arrowed in Fig. 1 ($\times 120$).

[To face p. 276

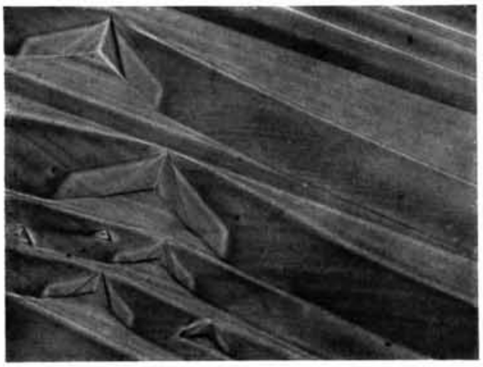

Fig. 3. Trigons with two wings (× 56).

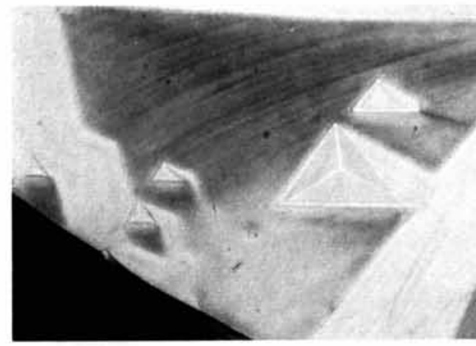

Fig. 4. Trigons with one wing (× 56).

Fig. 6. Multiplebeam interferogram on (111) face (× 80).

Fig. 7. Fringes of equal chromatic order (lower) and multiple-beam fringes (upper) on the region marked by an arrow in Fig. 6.

inclusions. It shows quite a strong birefringence, like most diamonds, thus indicating the presence of very considerable strain.

A similar habit is commonly observed in natural diamonds; however, the present crystal exhibits some peculiar and very clear surface features on both of the octahedral faces. These peculiar features are formed as a result of the combination of several vicinal faces which have grown on the octahedral faces.

For over nineteen years some thousands of diamonds, both natural and synthetic, have been examined in this laboratory and although surface features of the present kind have been noticed quite often, no detailed study has so far been made regarding the vicinal faces leading to them; nor as far as we know have scientific reports been published in this matter. Only Custers (1950) has reported on vicinal faces of fish-bone shape on an octahedral face of a coated natural diamond. According to his observations the direction of the edges of the vicinal faces is [123]. Here too we find this, but in addition to this direction, various other directions of the edges of the vicinal faces are found on the present diamond and an attempt is now made to associate the surface microtopographies with the habit change of the crystal.

Observations

The whole crystal is seen in Fig. 1 and a micrograph of the part indicated with an arrow is shown in Fig. 2. As may be seen in this picture a change in growth form occurs here.

The main octahedral faces of the crystal, which are more or less flat, show unusual features. These are formed by the combination of the familiar point-bottom trigon, but added are two wing-like vicinal faces attached to two sides of the triangular pattern, which being a trigon has a negative orientation (*i.e.* the three vertices of the triangular pattern point to the edges of the octahedral face, Fig. 3). In some instances only one wing pattern is attached to one side of the triangular pattern (Fig. 4).

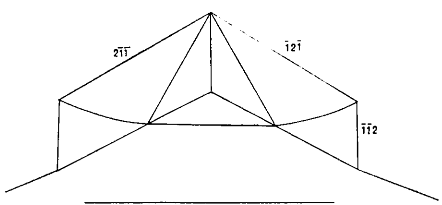

Fig. 5. Schematic drawing of a two-wing trigon.

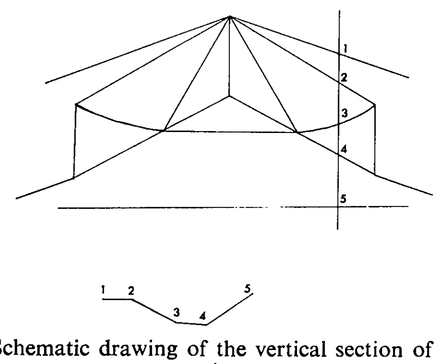

Fig. 8. Schematic drawing of the vertical section of the wing-trigon.

The main characteristic combinations of the vicinal faces in these patterns are shown in Fig. 5, where the indices of the edges are indicated.

The three edges are in three crystallographically related directions. By means of the light-profile method (Tolansky, 1953) and the fringes of equal chromatic order (Tolansky, 1960) it is established that the triangular patterns are point-bottomed type trigons with depths varying from less than $0{\cdot}3\mu$ up to 2μ.

We can conveniently refer to the trigons with two wing-like vicinal faces or one wing-like vicinal face as two-wing trigons or one-wing trigons respectively.

The actual topography of the face has been determined by several optical methods (light profile and fringes of equal chromatic order as already mentioned, and two-beam and multiple-beam interference fringes) (Tolansky, 1953, 1960). A fringe pattern is shown in Fig. 6. In this has been marked with an arrow one of the several regions on which we worked with the fringes of equal chromatic order, the example of which is shown in Fig. 7. (In this picture the upper patterns are multiple-beam Fizeau fringes appearing in the spectrograph with wide slit, for green and yellow mercury lines; the lower patterns are fringes of equal chromatic order.)

From the several pictures taken, it is possible to draw a schematic profile of the cross section of the wing trigons as shown in Fig. 8.

The topographies are much exaggerated in the vertical direction. Near the edge of the crystal it is found that when the opposite wings of two trigons join together they build up an $\{hkl\}$ form (with h almost equal to k) on the main (111) face (Fig. 9).

In addition to the main edges between the vicinal faces drawn schematically in Fig. 5, it is easy to detect many faint curved lines on these vicinal faces by means of a sensitive phase-contrast microscope (Olympus PMF). These faint curved lines do not intersect each other and they are presumably the edges of extremely thin layers. Judging from the visibility of these edges of the layers under the phase contrast (Figs. 3, 4, 9) and from the count of their number and the twist of the two beam interference fringes of Fig. 10, where the fringes of one wing are completely kinked, it is possible to estimate the step height of the extremely thin layers to be some tens of Ångstrom units. These faint lines, which are the edges of extremely thin layers, are here always observed on all vicinal faces of the crystal with the phase contrast microscope. In fact it is possible to say that every vicinal face seen here is formed by piling up of extremely thin layers on the octahedral face.

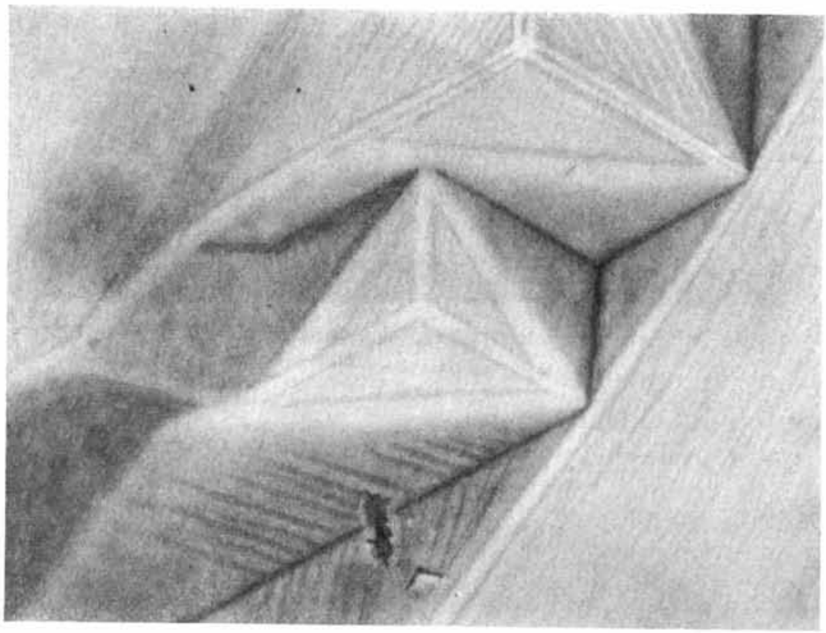

Fig. 9. Joining of the opposite wings of two wing-trigons (× 450).

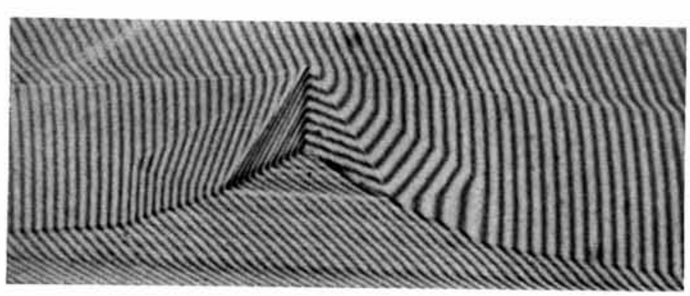

Fig. 10. Two-beam interferogram on a wing-trigon (× 130).

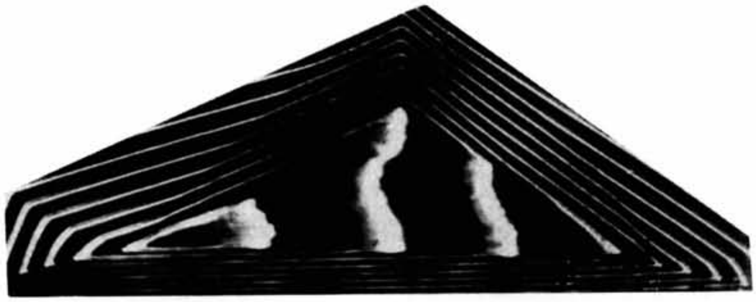

Fig. 11. Multiple-beam interferogram (high dispersion) on a trigon ($\times$ 125).

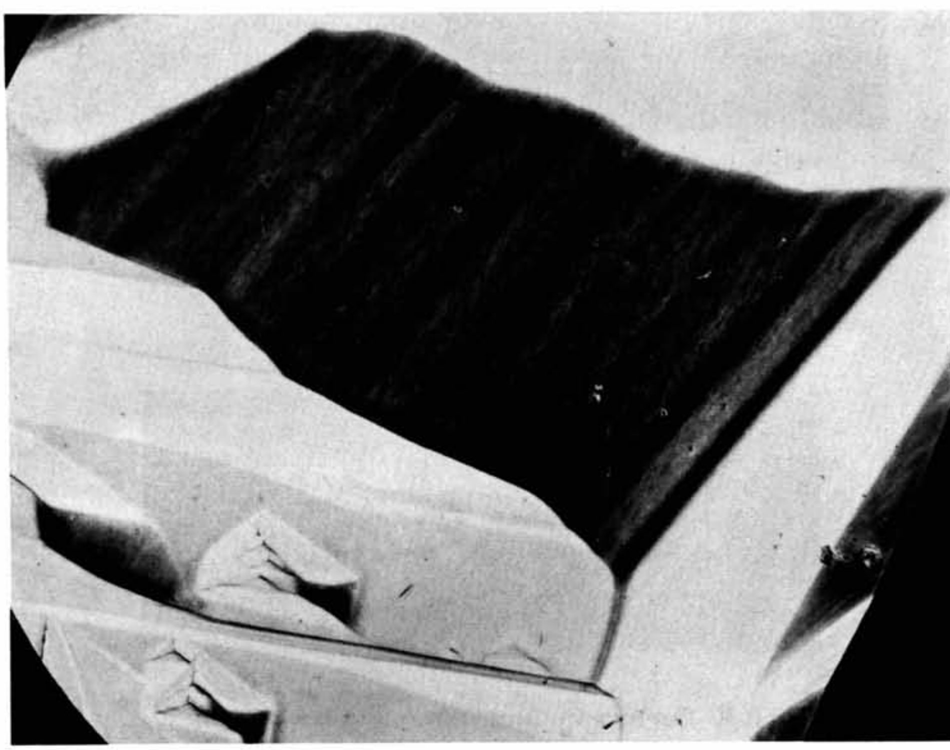

Fig. 12. Phase-contrast micrograph on the skirt faces of wing-trigons ($\times$ 110).

The notable features of the extremely thin layers show that there is a strict relation between these layers and the symmetrical shape of the wing trigons. As can be clearly seen in Fig. 3 the two-wing trigons can be divided into two equal portions which are situated in mirror image to each other with respect to a (110) type plane. We find that the directions of development of the thin layers on the wing trigons are also mirror images of each other with respect to the same plane described above, while in the case of one-wing trigons they are obviously asymmetrical shapes; and it is clearly shown in the micrograph (Fig. 4) that there is only one direction in the development of the thin layers.

In view of the several characteristics mentioned above one is readily led to assume that the thin layers are the growth layers which have progressed on the octahedral surfaces and formed those vicinal faces.

The wing trigons are distributed without any regularity and the sizes of the trigons vary with the depths, *i.e.* the deeper the bottom the larger the side. Interferometry with high-dispersion multiple-beam fringes shows also that the trigon has curved and kinked walls (Fig. 11).

As to the orientation of the wing trigons, it is interesting to note that they all have the same crystallographic orientation where they group together within a small part of the octahedral face. It is readily recognized that each octahedral face has five or six small regions where every wing trigon is in the same orientation in any particular region. These do, however, vary from part to part, being rotated at 60° to each other according to the symmetry of the (111) face on which they have grown.

The shapes of the wings are also modified by the relative rate of growth of the vicinal faces. For example the skirts of the wings in Fig. 12 (*i.e.* the dark parts) are more developed than the corresponding skirts in Fig. 3. The characteristic development of the skirts is remarkable in the case of Fig. 12. Judging from the reflectivity of light and the similar characteristic striation on the skirt faces, one can conjecture that the indices of the faces of the small skirts are almost the same as those of the large face. This will indicate that these small skirts have the potentiality of growing into large skirt faces indexed as (hkl) with h very near to k.

Discussion

It can be conjectured that there were at least two stages in the process of the crystal growth of this diamond. First was the formation of the flat $\{111\}$ form due to the extensive development of the two faces (111) and $(\bar{1}\bar{1}\bar{1})$; then followed the formation of new forms of the type $\{hkl\}$, the faces being very near to the form $\{hhl\}$ and at a later stage the form $\{hhl\}$ itself. It may happen that one face of the form $\{hkl\}$ may develop more than an adjacent one and the latter may later disappear, so that a new crystallographic form results. This is clearly seen in Fig. 9 where two wings have joined to build up an $\{hkl\}$ form, (since h is very near to k the line between (hkl) and (khl) faces is extremely faint). On the other side it may happen also that the second form may develop more and we arrive at the dark shapes of Fig. 12 which have almost the same index. The formation of the wing trigons may be contemporary with the above mentioned two stages of growth, so that a point-bottomed trigon may be formed at the first stage and the wings formed at a second stage.

As can be seen in several micrographs the larger the trigon the larger the wings both in lateral and vertical directions. This implies that the growth layers have piled up, surrounding the trigons to form the wings, and the growth layers have not filled up the trigons.

It is difficult to advance any hypothesis for the actual causes of the habit change, but one point is certain, namely that the habit change is related to the formation and propagation of the extremely thin layers of growth.

With regard to the hypothetical direction of flow of material, however, the orientation of the wing trigons could supply an answer, since it is observed that the interactions of the thin growth layers with a triangular pit (a trigon) have given rise to a wing trigon whose orientation is determined by the direction of the progress of the growth layer.

Taking this for granted, it is possible to say that there are several directions of flow of the material at the stage when the wings are formed on the octahedral faces. This should have affected to some extent the habit change of this crystal.

As to the habit change of the diamonds from the form $\{111\}$, in an ideal case of growth the following series of habit changes might be expected: $\{111\} \rightarrow \{hhl\} \rightarrow \{110\}$. From the present observations of the formation and the development of several vicinal faces the following sequence of growth forms is to be expected: $\{111\} \rightarrow \{hkl\} \rightarrow \{hhl\} \rightarrow \{110\}$.

We are very grateful to Professor S. Tolansky for his interest in the work, and for helpful suggestions.

One of us (F. B.) wishes to thank Professor E. Sanero for his constant support and the Consiglio Nazionale delle Ricerche for the grant of a NATO fellowship.

One of us (H. K.) gladly aknowledges receipt of a British Council scholarship.

References

Custers, J. F. H. (1950). *Amer. Min.* **35**, 51.

Tolansky, S. (1953). *Specialized Microscopical Techniques in Metallurgy*. London: The Institute of Metals.

Tolansky, S. (1960). *Surface Microtopography*. London: Longmans.